THE COMPANY OF
Biologists

RESEARCH ARTICLE

The sensitivity of lateral line receptors and their role in the behavior of Mexican blind cavefish (*Astyanax mexicanus*)

Masato Yoshizawa[1,‡], William R. Jeffery[1], Sietse M. van Netten[2] and Matthew J. McHenry[3,*]

ABSTRACT

The characid fish species *Astyanax mexicanus* offers a classic comparative model for the evolution of sensory systems. Populations of this species evolved in caves and became blind while others remained in streams (i.e. surface fish) and retained a functional visual system. The flow-sensitive lateral line receptors, called superficial neuromasts, are more numerous in cavefish than in surface fish, but it is unclear whether individual neuromasts differ in sensitivity between these populations. The aims of this study were to determine whether the neuromasts in cavefish impart enhanced sensitivity relative to surface fish and to test whether this aids their ability to sense flow in the absence of visual input. Sensitivity was assessed by modeling the mechanics and hydrodynamics of a flow stimulus. This model required that we measure the dimensions of the transparent cupula of a neuromast, which was visualized with fluorescent microspheres. We found that neuromasts within the eye orbit and in the suborbital region were larger and consequently about twice as sensitive in small adult cavefish as in surface fish. Behavioral experiments found that these cavefish, but not surface fish, were attracted to a 35 Hz flow stimulus. These results support the hypothesis that the large superficial neuromasts of small cavefish aid in flow sensing. We conclude that the morphology of the lateral line could have evolved in cavefish to permit foraging in a cave environment.

KEY WORDS: Neuromast, Adaptive behavior, Cupula, Hydrodynamics, Convergent evolution, Sensory evolution

INTRODUCTION

The evolution of sensory systems can be crucial for an animal to adapt to a new environment. An intriguing example is offered by *Astyanax mexicanus* (De Filippi 1853), a species that includes cave-dwelling and ancestral-type stream-dwelling populations (Bradic et al., 2012; Gross, 2012; Ornelas-García et al., 2008). The cavefish became blind as they migrated into caves within the past few million years, whereas stream-dwelling populations (i.e. 'surface fish') retained a functional visual system. Comparisons between these populations of Mexican blind cavefish provide insight into the evolutionary changes caused by a radical alteration in habitat (Jeffery, 2001; Jeffery, 2009; Mitchell et al., 1977; Wilkens, 1988). One of the most dramatic changes occurred in the lateral line system of cavefish, which has receptors that cover the skin at a high density

[1]Department of Biology, University of Maryland, College Park, MD 20742, USA. [2]Department of Artificial Intelligence and Cognitive Engineering, University of Groningen, 9747 AG Groningen, The Netherlands. [3]Department of Ecology and Evolutionary Biology, University of California, Irvine, Irvine, CA 92697, USA. ‡Present address: Department of Biology, Univeristy of Nevada, Reno, NV 89557, USA.

*Author for correspondence (mmchenry@uci.edu)

compared with surface fish (Schemmel, 1967; Teyke, 1990; Yoshizawa et al., 2010; Yoshizawa et al., 2012a). These receptors, known as superficial neuromasts, detect water flow in both populations, but perhaps with different sensitivity. The aims of the present study were to evaluate whether the superficial neuromasts of cavefish are more sensitive than those of surface fish and to test whether cavefish have a superior ability to sense oscillations in the water column.

Cavefish exhibit an ability to detect flow when they are attracted to an object that oscillates at the water's surface. This vibration attraction behavior (VAB) is mediated by superficial neuromasts within the eye orbit (EO). In blind fish, these neuromasts are found dorsal to the infraorbital canal, at a position where the eye resides in a sighted fish. Therefore, these neuromasts are anatomically distinct from infraorbital canal neuromasts (Schemmel, 1967; Yoshizawa et al., 2012b). The number of EO neuromasts is genetically correlated with the level of VAB in F_2 and F_3 hybrids from a surface fish and Pachón cavefish cross (Yoshizawa et al., 2012b). However, no detectable correlation exists for the neuromasts in an adjacent region on the cranium, the third infraorbital bone (IO-3, previously denoted as the third suborbital bone, SO-3) (Yoshizawa et al., 2010; Yoshizawa et al., 2012a; Yoshizawa et al., 2012b). An experimental ablation of EO neuromasts causes cavefish to decrease VAB significantly, whereas the same treatment for IO-3 neuromasts shows no effect (Yoshizawa et al., 2012b). This demonstrates a major role of EO neuromasts on VAB. The present study examined differences in the sensitivity of EO neuromasts in comparison with IO-3 neuromasts in both surface fish and cavefish.

The morphology of a neuromast has the potential to influence VAB through its frequency-dependent sensitivity. The neuromast includes a transparent extracellular structure, the cupula, which surrounds the hair bundles that project from the apical surfaces of hair cells within the sensory epithelium. Each hair bundle includes a non-motile kinocilium and a stair-step arrangement of microvilli (i.e. stereocilia) that provides the site of mechanotransduction (Hudspeth, 1982) and functions as a spring-like connection between the cupula and the epithelium (van Netten and Kroese, 1987). In superficial neuromasts, the cupula is elongated and bends in flow over the surface of the body (Dinklo, 2005). This bending is generated by the drag on the cupula, which increases with distance from the surface due to the boundary layer, inducing a spatial gradient in flow. Largely as a result of this effect, a taller cupula endows a neuromast with greater sensitivity (McHenry et al., 2008; Teyke, 1988; Teyke, 1990). However, height alone does not dictate sensitivity because neuromasts with greater numbers of hair bundles, or a wider cupula, possess a greater flexural stiffness that reduces sensitivity (McHenry and van Netten, 2007). Therefore, a full consideration of the sensitivity of a neuromast must take into account the morphological features that affect both fluid and structural dynamics.

The present study employed novel theoretical and experimental approaches to examine the morphology and sensitivity of superficial

Table 1. ANOVA statistics for morphological variables

Variable	w				h				n			
	SS	d.f.	F	P	SS	d.f.	F	P	SS	d.f.	F	P
Population	1527	2	34.9	<<0.001	16,066	2	18.6	<<0.001	2678	2	20.9	<<0.001
Position	35.1	1	1.6	0.2	2362	1	5.46	0.02	130	1	2.03	0.16
Age	1232	1	56.4	<<0.001	1594	1	3.68	0.06	3763	1	58.7	<<0.001
Population × position	19.1	2	0.44	0.65	696.8	2	0.81	0.45	111	2	0.86	0.42
Population × age	271	2	6.21	<0.01	7634	2	8.82	<<0.001	759	2	5.92	<0.01
Position × age	37.5	1	1.72	0.19	691	1	1.60	0.21	140	1	2.19	0.14
Error	2272	104			45,003	104			6665	104		
Total	6424	113			88,907	113			1634	113		

d.f., degrees of freedom; F, F-statistic; h, height; n, no. hair cells; population, Los Sabinos, Pachón, surface; position of cupula, IO-3 or EO; age, small or large; SS, sum of squares; w, cupula width.

neuromasts. This introduces new techniques for visualizing the cupula of the neuromast, with improved contrast (McHenry and van Netten, 2007; Teyke, 1990), and an analytical model of the micromechanics of neuromasts. Our analysis focused on a comparison of surface fish with cavefish from two populations (Los Sabinos and Pachón). These two groups of cavefish evolved an increase in the number of superficial neuromasts by distinct sets of genes, which suggests convergent evolution between these populations (Bradic et al., 2012; Dowling et al., 2002; Ornelas-García et al., 2008) and involvement of different genes with opposing directions of parental genetic effects (i.e. maternal or paternal genetic effects) (Yoshizawa et al., 2012a). We compared neuromasts and VAB between small and large adults as an additional means to evaluate their relationship because neuromast size decreases with growth in this species (Teyke, 1990).

RESULTS
Neuromast morphology and sensitivity
Neuromast cupulae were found to vary with age and population, with a high degree of significance (P<<0.001, Table 1). *Post hoc* comparisons demonstrated that the cupula was significantly larger in width (Fig. 1A) and height (Fig. 1B) for cavefish (Los Sabinos and Pachón) than for surface fish in both EO and IO-3 neuromasts for both small and large individuals (width), or small individuals (height). The greatest differences were found in small fish. For example, the median height of EO cupulae in Los Sabinos (75 μm, N=4) and Pachón (76 μm, N=4) populations was more than twice that of small surface fish (31 μm, N=4, Fig. 1B). Cupula height for IO-3 was indistinguishable from that for EO, and median values for Los Sabinos (96 μm, N=23) and Pachón (89 μm, N=16) populations were also about twice that of young surface fish (48 μm, N=15, the second right panel of Fig. 1B). The aspect ratio (Fig. 1C) followed similar variation among groups to cupula height, which indicates that taller cupulae were generally more elongated because of a disproportionately greater height with modest differences in width.

The number of hair cells was also found to be significantly different between fish of different populations and age (P<<0.001), with an interactive effect between these factors (P<0.01, Table 1). Surface fish consistently possessed neuromasts with fewer hair cells than cavefish from both populations and large individuals possessed neuromasts with more hair cells than small individuals in most *post hoc* comparisons (Fig. 1D). The noteworthy differences between cavefish and surface fish were found in small fish. For EO neuromasts, hair cells were more numerous in Los Sabinos (median 38 hair cells, N=4) than in Pachón (28 hair cells, N=4), which had more hair cells than surface fish (17 hair cells, N=4).

The dimensions of the cupula and number of hair cells had consequences for the micromechanics of neuromasts, as interpreted by our mathematical model. The population and age of the fish exhibited highly significant (P<<0.001) effects on all mechanical parameters that were considered (Table 2). The causes of these effects and the interactions between factors were explored with *post hoc* comparisons. One component of sensitivity, the compliance parameter (K_{comp}; Fig. 2A), was relatively high in small surface fish, but this was more than offset by relatively small values in the low-frequency (K_{low}; Fig. 2B) and high-frequency (K_{high}; Fig. 2C) parameters. For example, the compliance parameter for IO-3 neuromasts for small surface fish (median 3800 $s^2\,kg^{-1/2}\,m^{-3/2}$, N=14) was more than 50% greater than that for Pachón (2400 $s^2\,kg^{-1/2}\,m^{-3/2}$, N=16) and almost twice that of Los Sabinos fish (2000 $s^2\,kg^{-1/2}\,m^{-3/2}$, N=23, Fig. 2A). However, the low-frequency parameter for the same neuromast in surface fish (median 76.0 $s^{-1/2}\,kg^{1/2}\,m^{3/2}$, N=14) was less than one-third the value for Pachón (250.5 $s^{-1/2}\,kg^{1/2}\,m^{3/2}$, N=16) and about one-quarter that of Los Sabinos (291.0 $s^{-1/2}\,kg^{1/2}\,m^{3/2}$, N=23, Fig. 2B). The high-frequency parameter for this neuromast in surface fish (median 0.45×10^{-9} $s^{-1}\,kg^{1/2}\,m^{3/2}$, N=14) was comparably smaller than that of the cavefish (Los Sabinos: 1.75×10^{-9} $s^{-1}\,kg^{1/2}\,m^{3/2}$, N=23; Pachón: 1.37×10^{-9} $s^{-1}\,kg^{1/2}\,m^{3/2}$, N=16, Fig. 2C). Therefore, the sensitivity at both low and high frequencies (Eqns 6 and 7) for surface fish is predicted to be substantially lower than that of cavefish. In contrast, the cut-off frequency varied by over three orders of magnitude in all cases, but showed no significant effects of population, age or cupula position (Fig. 2D).

These differences in mechanical properties were predicted by our mathematical model to influence the frequency response of neuromasts. We calculated the frequency response (Eqn 1) using the third-quartile values for mechanical parameters as a means of examining high-end sensitivity within each group. For the EO neuromasts, small cavefish exhibited substantially greater sensitivity at all frequencies (Fig. 3A) and these differences were similar for IO-3 neuromasts (Fig. 3B). Large surface fish exhibited greater sensitivity at most frequencies for both EO and IO-3 neuromasts than smaller fish. In contrast, it was generally the smaller fish that had greater sensitivity in both Pachón and Los Sabinos cavefish (Fig. 3). As described below, the distribution of the sensitivity predicted for a 35 Hz stimulus was further considered in comparison to behavioral experiments conducted with a vibration stimulus of that frequency.

Vibration attraction behavior
Small cavefish exhibited a different response to a hydrodynamic stimulus than surface fish. This trend was most apparent in the maximum and third-quartile values of VAB, as indicated by the number of approaches toward a vibrating rod (Fig. 4A,B). These
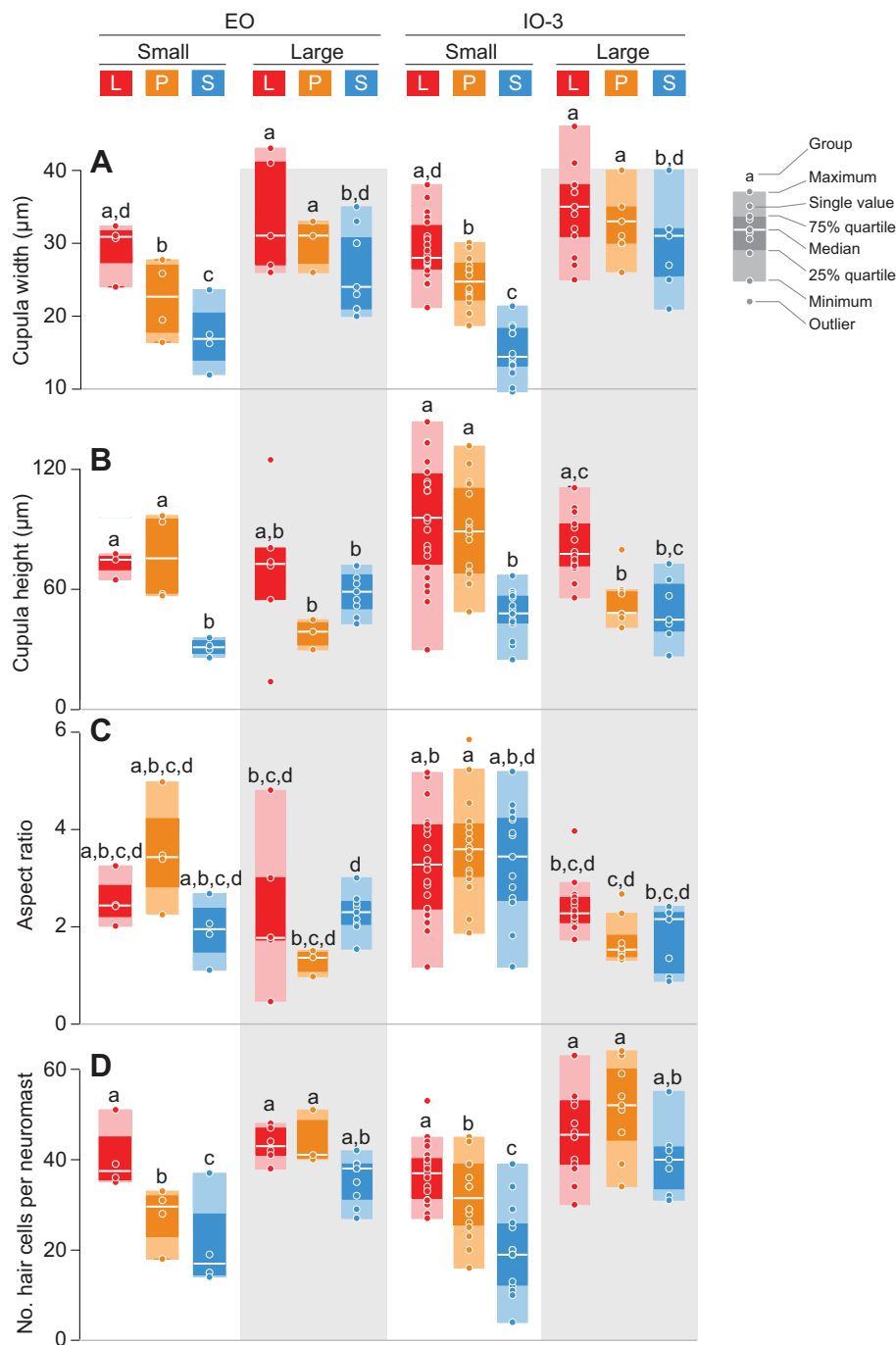
Fig. 1. The morphometrics of superficial neuromasts. The major dimensions of the cupula and number of hair cells were measured in individuals from Los Sabinos (L, red), Pachón (P, orange) and surface fish (S, blue) populations for EO (left column) and IO-3 (right column) superficial neuromasts in small and large adults (gray columns). The key illustrates the symbols for individual measurements (circles), the range of values (light rectangle), the bounds of the first (25%) and third (75%) quartiles (dark rectangle) and the median (white line). Outliers were identified as exceeding 50% of the range between the first and third quartiles. Statistical groups are designated by letters, with groups distinguished as significantly different, as determined by *post hoc* testing. Each fish studied provided up to one neuromast of each type; therefore, each value in a plot represents a distinct individual.

values increased at higher stimulus frequencies, up to 35 Hz. Beyond this rate, the number of approaches declined monotonically with stimulus frequency. In contrast, surface fish did not approach the stimulus with a number of approaches any greater than when the rod was motionless (Fig. 4C).

For VAB measurements to a 35 Hz stimulus, age and population were significant factors on both behavior and the mechanical sensitivity of a neuromast (Table 3, Fig. 5). In small adults, the median number of approaches in Los Sabinos (16, *N*=16) and Pachón (25, *N*=19) fish was many times greater than in surface fish (3, *N*=19). Also, in small adults, the median values for sensitivity in both types of neuromasts for Los Sabinos (1.67 μs for EO, *N*=4; 2.29 μs for IO-3, *N*=23) and Pachón (1.69 μs for EO, *N*=4; 2.17 μs for IO-3, *N*=16) fish were about twice that of surface fish (0.88 μs for EO, *N*=4;

0.98 μs for IO-3, *N*=14), and the two types of neuromast were not significantly different from each other. These differences in the sensitivity were aligned well with the VAB levels between cavefish and surface fish, and between small and large fish, except Los Sabinos cavefish. Los Sabinos fish possessed almost the same sensitivity between small and large fish, although large fish did not exhibit VAB (number of approaches >4) (Yoshizawa et al., 2010).

DISCUSSION

Our results suggest that blind cavefish possess neuromasts that are more sensitive than those of surface fish, principally because they are larger. This likely contributes to the ability of these animals to detect oscillatory flow, which is a likely benefit for foraging in a cave environment (Bleckmann et al., 1991; Lang, 1980). To our

Table 2. ANOVA statistics for mechanical variables

	K_{comp}				K_{low}				K_{high}			
Variable	SS	d.f.	F	P	SS	d.f.	F	P	SS	d.f.	F	P
Population	2.57×10^7	2	19.9	<<0.001	3.43×10^5	2	14.0	<<0.001	1.93×10^{-17}	2	24.9	<<0.001
Position	2.16×10^5	1	0.33	0.56	4.83×10^4	1	3.94	0.05	6.32×10^{-19}	1	1.63	0.20
Age	2.58×10^7	1	39.9	<<0.001	4.84×10^4	1	3.95	0.05	1.74×10^{-17}	1	44.9	<<0.001
Population × position	3.59×10^5	2	0.28	0.76	1.88×10^4	2	0.77	0.47	2.28×10^{-19}	2	0.29	0.75
Population × age	1.42×10^7	2	11.0	<<0.001	1.32×10^5	2	5.37	<0.01	1.49×10^{-18}	2	1.92	0.15
Position × age	1.31×10^5	1	0.20	0.65	2.71×10^4	1	2.21	0.14	5.96×10^{-18}	1	1.53	0.23
Error	6.66×10^7	103			1.26×10^6	103			4.00×10^{-17}	103		
Total	1.46×10^8	112			2.23×10^6	112			9.21×10^{-17}	112		

d.f., degrees of freedom; F, F-statistic; K_{comp}, compliance parameter; K_{low}, low-frequency parameter; K_{high}, high-frequency parameter; population, Los Sabinos, Pachón, surface; position of cupula, IO-3 or EO; age, small or large; SS, sum of squares.

knowledge, this is the first demonstration of a relationship between superficial neuromast morphology and fish behavior. This supports the idea that differences in neuromast sensitivity created by morphological evolution (eye regression) contributed to sensory and behavioral changes via genetic assimilation (Yoshizawa et al., 2012b; Rohner et al., 2013).
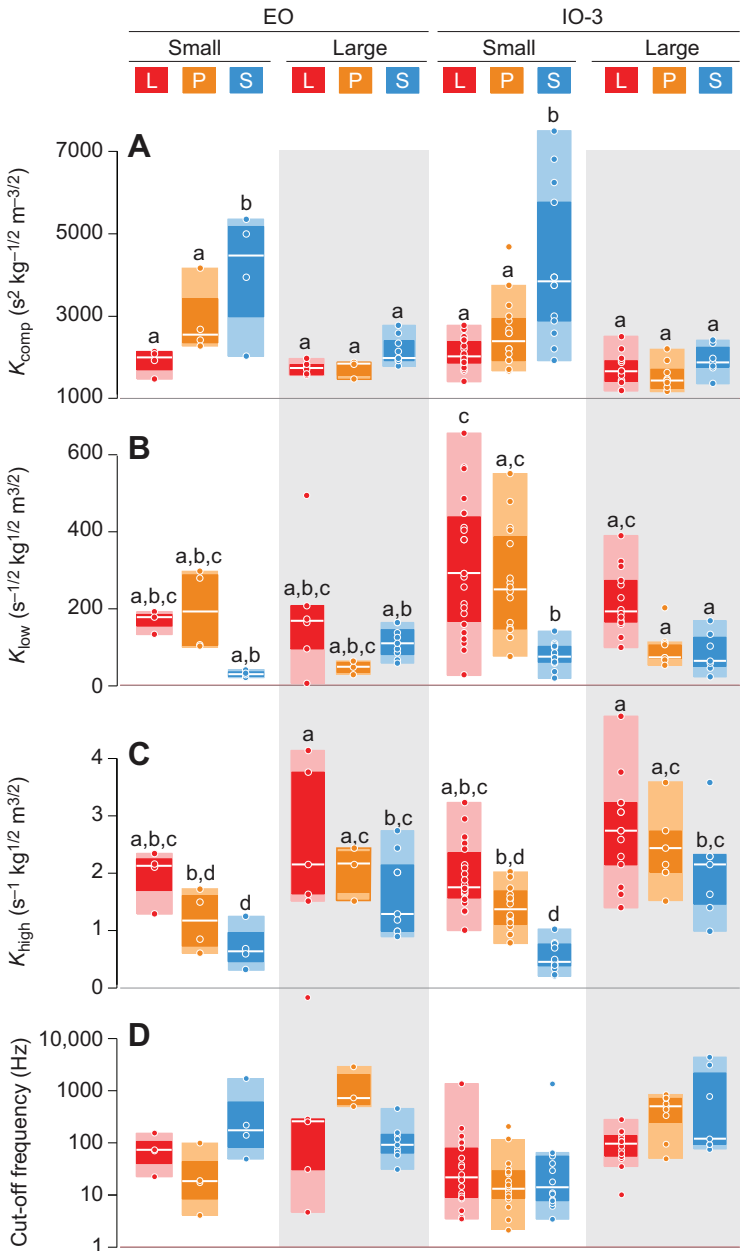

Fig. 2. Micromechanical properties of superficial neuromasts, as defined by the mathematical model (Eqn 1). (A) For all stimulus frequencies, the sensitivity of a neuromast is proportional to the compliance parameter (K_{comp}; Eqn 2), which indicates the magnitude of the material stiffness of the cupula relative to the spring stiffness of the hair bundles. (B) Sensitivity is proportional to the low-frequency parameter (K_{low}; Eqn 3) for stimulus frequencies below the cut-off frequency, and (C) proportional to the high-frequency parameter (K_{high}; Eqn 4) for frequencies above the cut-off. (D) The cut-off frequency is determined by the relative magnitude of the low- and high-frequency parameters (Eqn 5). All symbol definitions are provided in Fig. 1.
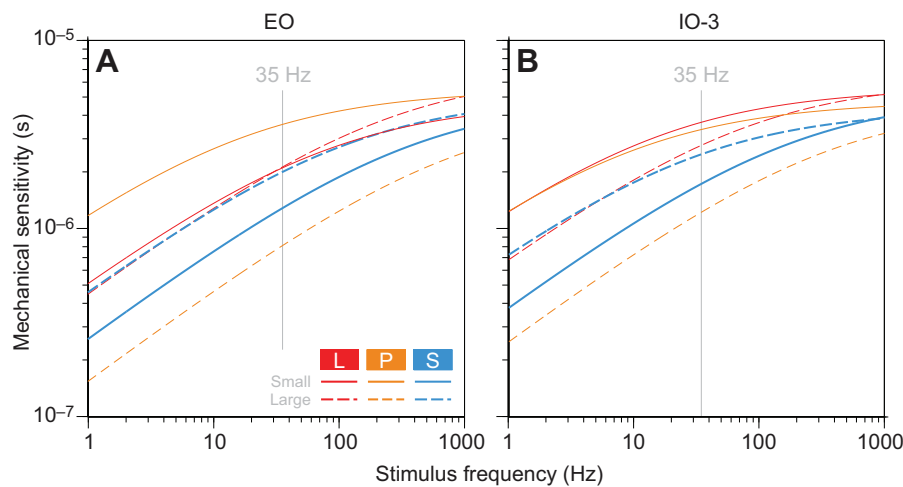
Fig. 3. The frequency response of superficial neuromasts, as predicted by our micromechanical model. Calculations were performed using the third quartile of mechanical parameter values (Fig. 2), and therefore represent a sampling of high sensitivity from each group. Mechanical sensitivity is defined as the amplitude of the ratio of hair bundle deflection to free-stream velocity (i.e. the absolute value of Eqn 1) for small (solid lines) and large adults (dashed lines) of the Los Sabinos (L, red), Pachón (P, orange) and surface (S, blue) populations. These frequency responses were calculated for (A) EO and (B) IO-3 superficial neuromasts.

Our mathematical model demonstrates how the larger cupulae of neuromasts in small cavefish enhances the sensitivity of the lateral line system. The model accounts for the filtering generated by the boundary layer flow over the surface of the body and the beam mechanics of the cupula to predict the deflection of the hair cells in a neuromast (McHenry et al., 2008; van Netten and McHenry, 2013) (G. C. Sendin, P. Pirih, T. Dinko and S.M.v.N., in preparation). It determined that the mechanical sensitivity for cavefish is about twice that of surface fish for a stimulus of 35 Hz in small adults (Fig. 5B,C). This result stems from the frequency response of the neuromasts. A 35 Hz stimulus is generally below the cut-off frequency (Fig. 2D) in the high-pass filtering of a superficial neuromast (Fig. 3). In this low-frequency domain, mechanical sensitivity is proportional to the low-frequency parameter (Eqn 6), which is proportional to the square of cupula height (Eqn 5). Therefore, the taller cupula of a small cavefish (Fig. 1B) endows the neuromasts with greater low-frequency sensitivity than in surface fish (Fig. 2B). Teyke similarly suggested that the elongated cupulae of cavefish provide enhanced sensitivity (Teyke, 1990). Teyke's study reported measurements of cupula height (~150 μm) for *A. hubbsi*, which is the same as the Los Sabinos population of *A. mexicanus* studied here (Mitchell et al., 1977). The neuromasts
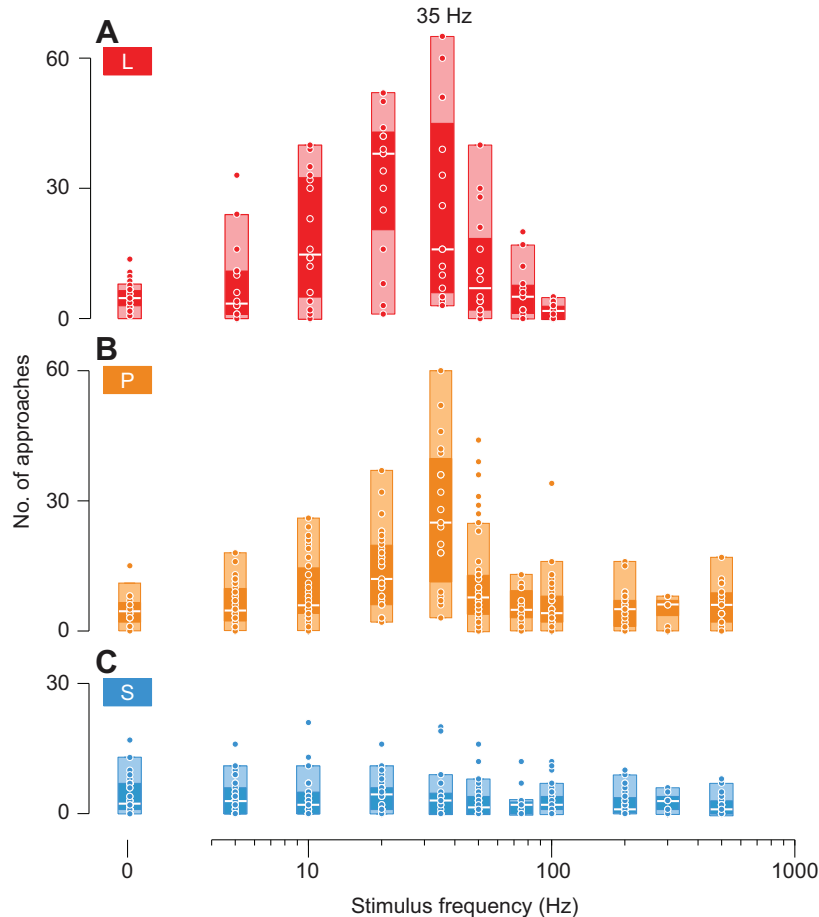
Fig. 4. Vibration attraction behavior. The number of instances in which individuals approached a vibration rod at the surface of the water varied with stimulus frequency in the blind cavefish from (A) Los Sabinos (L, red) and (B) Pachón (P, orange) populations, but not in (C) surface fish (S, blue). Variation in behavior is only apparent in the maximum and third quartile values. All symbol definitions are provided in the legend for Fig. 1.

Table 3. ANOVA statistics for behavior and neuromast sensitivity at 35 Hz

Variable	AP				S			
	SS	d.f.	F	P	SS	d.f.	F	P
Population	2680	2	9.71	<<0.001	7.10×10^{-12}	2	10.3	<<0.001
Position					1.43×10^{-12}	1	4.14	0.04
Age	7000	1	50.6	<<0.001	3.15×10^{-12}	1	9.15	<<0.001
Population × position					8.10×10^{-13}	2	1.17	0.31
Population × age	2400	2	8.83	<<0.001	5.88×10^{-12}	2	8.53	<0.01
Position × age					4.47×10^{-13}	1	1.30	0.26
Error	12,700	92			3.55×10^{-11}	103		
Total	25,365	94			6.36×10^{-11}	112		

AP, approach frequency; d.f., degrees of freedom; F, F-statistic; population, Los Sabinos, Pachón, surface; position of cupula, IO-3 or EO; age, small or large; S, mechanical sensitivity; SS, sum of squares.

considered may have been from a different cranial location (e.g. the supraorbital area) than our measurements, which could account for the larger values.

In the present study, neuromasts at different locations around the eye were found to vary in a similar manner. For each population and age group, EO neuromasts were indistinguishable from IO-3 neuromasts in their morphometrics (Fig. 1) and mechanical sensitivity (Fig. 2). This result may not have been expected, given the major role of EO neuromasts for VAB (Yoshizawa et al., 2012b). If neuromast morphology evolved to heighten sensitivity in cavefish (Yoshizawa et al., 2010; Yoshizawa et al., 2012b; Yoshizawa et al., 2013), then it appears to have occurred in more than just the EO location. The heightened influence of these neuromasts on behavior must be attributable to factors other than their mechanical sensitivity. For example, the central nervous system may be particularly responsive to stimuli detected by EO neuromasts or unrevealed orientations of directional sensitivity (Coombs et al., 1989) of EO neuromasts may play a major role in VAB.

Responsiveness to oscillatory stimuli does not appear to persist as cavefish grow because VAB is not exhibited in large adults (Fig. 5A). We found this lack of attraction to oscillations in large Los Sabinos fish despite the fact that they exhibited no difference in sensitivity from small fish (Fig. 5B,C). Therefore, the loss of VAB must be attributed to a change in the nervous system. This could be related to a change in foraging behavior over the life history of the cavefish, such as might occur by resource partitioning between life history stages. Alternatively, this result could be an artifact of lab rearing. For example, the large adults may have learned that they can better acquire food by responding to olfactory (Menuet et al., 2007) or auditory cues, rather than oscillatory flow when fed in aquaria. Large Pachón cavefish also showed no VAB (Fig. 5A), but they were also found to have neuromasts that were less sensitive (Fig. 5B,C). Therefore, neuromast sensitivity could be a contributor to the loss of VAB in these fish. The disappearance of VAB in large cavefish may also be due to the lower density of neuromasts compared with smaller fish (Fig. 6) (Schemmel, 1967; Teyke, 1990; Yoshizawa et al., 2010; Yoshizawa et al., 2012a).

Our measurements were enabled by a novel visualization technique. Research on the functional morphology of the lateral line system has been hampered by traditional visualization techniques. Preparation for scanning electron microscopy destroys the cupulae of the neuromasts (Webb, 1989) and vital stains such as Methylene Blue (Teyke, 1990) and polystyrene microspheres (McHenry and van Netten, 2007) yield low contrast for resolving the dimensions of the cupula at high magnification. The present study improved contrast by using fluorescent polystyrene microspheres (Figs 6, 7), which preferentially adhere to the cupula material. This allows unprecedented insight into

the morphology of the cupula and measurements of the features that are essential for a prediction by a biophysical model (Eqn 1).

In summary, we present here a first survey of the cupula morphometrics in the superficial neuromasts of *Astyanax* surface fish and cavefish and its correlation with foraging behavior. Through a mathematical model, we found that two genetically distinct cavefish populations posses a higher sensitivity of the lateral line system than surface fish and are capable of detecting oscillations in flow. Our comparative approach has necessarily been limited to two cavefish populations, but could be enhanced by a broader survey of the 29 known cavefish populations (Mitchell et al., 1977; Yoshizawa et al., 2010). Future investigations could explore this diversity to examine how lateral line-mediated behavior has evolved within this intriguing group of animals.

MATERIALS AND METHODS
Animals
All individuals of *A. mexicanus* were laboratory-raised descendants of fish collected from the field. In cavefish, VAB level in lab-reared fish was previously shown to be slightly lower than in wild-caught fish, with no obvious difference in neuromast number (Yoshizawa et al., 2010). Surface fish were originally collected from Balmorhea Springs State Park, TX, USA. Cavefish were originally collected from Mexico in Cueva de El Pachón (Pachón cavefish) in Tamaulipas, and Cueva de los Sabinos (Los Sabinos cavefish) in San Luis Potosí (Jeffery, 2001; Jeffery and Martasian, 1998; Yamamoto and Jeffery, 2000; Yamamoto et al., 2003; Yoshizawa and Jeffery, 2008; Yoshizawa et al., 2012a). All subjects in the present study were adults that we categorized as 'small' if less than 4 cm in standard length and 'large' if greater than 6 cm. The small fish were between 1 and 2 years in age and the large fish were older than 3 years. Small fish were fed live *Artemia* larvae and maintained in groups of ~10 in 3 l tanks, which limits space to grow (Gallo and Jeffery, 2012). Large fish were fed TetraMin Pro Tropical Crisps flake food (Tetra Inc., Melle, Germany) and maintained in 38 l tanks. All experimental procedures were approved by the University of Maryland Animal Care and Use Committee and conform to NIH guidelines.

Cupula visualization
The cupula of a neuromast is an extracellular matrix with a refractive index close to that of water, but can be visualized with latex microspheres (McHenry and van Netten, 2007; Van Trump and McHenry, 2008). We enhanced the contrast of the cupula images by the use of fluorescent microspheres (0.10 μm Fluoresbrite YG Microspheres, Polysciences, Inc., Warrington, PA, USA). This was achieved by slowly exposing a fish to a ~1 ml solution of microspheres (1 drop in 2 ml of water) using a 2 μl Eppendorf tip when the fish was anesthetized with ice-cold Ringer's solution (1.77 mmol l^{-1} CaCl$_2$, 116 mmol l^{-1} NaCl, 2.9 mmol l^{-1} KCl, 10 mmol l^{-1} Hepes, pH 7.2). The fish were washed with this water, and cupulae were visualized at low magnification using a fluorescence microscope (Zeiss Axioskop2 with 2.5×Plan-Neofluor lens and a GFP filter set, Zeiss,
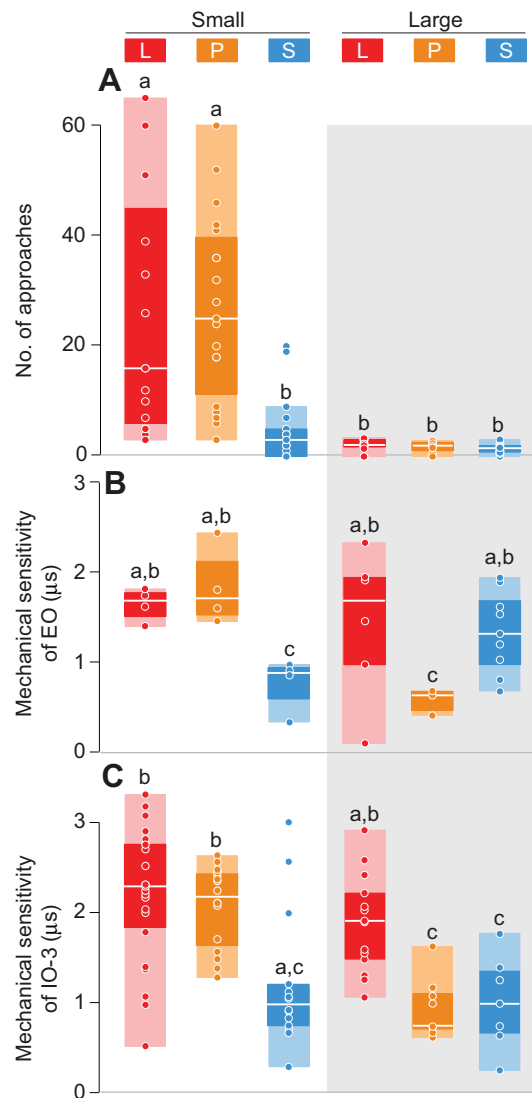
Fig. 5. Behavioral and neuromast sensitivity to a 35 Hz stimulus.
(A) Measurements for the approach frequency of the vibration attraction behavior are plotted with the predictions of mechanical sensitivity (Eqn 1) for the (B) EO and (C) IO-3 superficial neuromasts. Sets of measurements are provided for small (left column) and large adults (right column, in gray) of Los Sabinos (L, red), Pachón (P, orange) and surface (S, blue) populations. All symbol definitions are provided in the legend for Fig. 1. Statistical groups were shared between neuromasts (B,C), but were distinct from VAB measurements (A).

Göttingen, Germany). Individual neuromasts were visualized at high magnification with a motorized compound microscope (Zeiss Axioplan2 with a FITC-filter with 40×AchroPlan water-immersion) using both Nomarski (for hair cells) and fluorescence (for the cupula) illumination. We prepared the cranial skin by first removing the iridophore layer (medial to the cranial bone) and then transferring the preparation to Leibovitz's L-15 medium with 10% fetal bovine serum (Life Technologies Corp., Grand Island, NY, USA) reserved in a custom-made cup (made of Peel-A-Way Disposable Histology Molds, 22×22×20 mm width×height×depth; Polysciences, Inc.) that was glued to a pre-cleaned glass slide. A drop of 3% methylcellulose in Ringer's solution was used to mount the skin specimen on the surface of the slide. Photographs of cupulae at low and high magnifications were taken with a Zeiss AxioCam HRc CCD camera. For morphometric measurements, we photographed the neuromast along its height at regular (1 or 1.5 μm) intervals by focusing through the cupula (Fig. 7). We imaged superficial neuromasts both in the epidermis over the

cranial third infraorbital (IO-3) bone (Yamamoto et al., 2003) and within the nearest IO-3 area of the orbit epidermis dorsal to, and around, the line of the infraorbital canal, which was visualized under DIC (indicated by a yellow dashed line in Fig. 6). The infraorbital canal neuromasts were not stained with fluorescent microspheres in this short-time application. A single neuromast of each type was visualized to acquire morphometric measurements in each individual fish.

Morphometrics
We used high-magnification images of individual neuromasts to measure features of mechanical significance. As detailed below ('Mathematical model'), a number of morphological parameters are required to model the micromechanical properties of a neuromast. As previously described (Teyke, 1988), the hair bundles covered a region of the sensory epithelium that was approximately circular in shape, with projections of the gelatinous cupula in a direction perpendicular to the axis of sensitivity. We measured the cupula height (i.e. the distance between the superficial epithelium and cupula tip), width (i.e. the thickness of the cupula at the surface of the epithelium in the direction of hair cell sensitivity) and number of hair cells. These features were measured using images that were automatically scaled to the optics of the motorized microscope with Zeiss software (Axioplan2 with AxioVision v. 4.7).

Mathematical model
We used a mathematical model of the micromechanics of a superficial neuromast to determine the functional implications of morphological differences. This model was originally proposed in a form that required numerical solutions (McHenry et al., 2008), was recently modified (van Netten and McHenry, 2013) (G. C. Sendin, P. Pirih, T. Dinko and S.M.v.N., in preparation), and is presented here in a completely analytical form. This allows an interpretation of the effect of morphological parameters on neuromast sensitivity. The model predicts the mechanical sensitivity of a neuromast S (s), defined as the ratio of hair bundle deflection to stimulus velocity. It considers the boundary layer flow created by an oscillating pressure field next to the surface of the body (McHenry et al., 2008; Teyke, 1988). The model additionally considers the beam mechanics of the cupula and hair bundles that resist the drag generated by the boundary layer flow. The present formulation assumes boundary conditions with zero linear or angular displacement at the base of the cupula and no bending moment or shear force at the distal end of the cupula. These dynamics produce a frequency response that is articulated by the following equation, which is in complex notation:

$$S(f) = K_{low} K_{comp} \frac{\sqrt{2if}}{1 + \left(\frac{K_{low}}{K_{high}} \right) \sqrt{2if}}, \quad (1)$$

where f is the stimulus frequency. This equation predicts low-pass filtering by the hydrodynamics and mechanics of the neuromast and does not incorporate any filtering by the transduction of the hair cells and encoding by the afferent neurons.

According to this model, three mechanical parameters determine the sensitivity of a neuromast. The compliance parameter, K_{comp} ($s^2 kg^{-1/2} m^{-3/2}$), is inversely related to the spring stiffness of a hair bundle (k=1 mN m^{-1}) (Géléoc et al., 1997; McHenry et al., 2008) in the following manner:

$$K_{comp} = \frac{2.37 \sqrt{\rho}}{nk}, \quad (2)$$

where ρ is the density of water as well as that of the cupula and n is the number of hair cells. As indicated by Eqn 1, sensitivity at all frequencies varies directly with the compliance parameter. The dimensionless numerical value of 2.37 was found to agree well with measurements of neuromast deflection (Dinklo, 2005; McHenry et al., 2008). The low-frequency parameter, K_{low} ($s^{-1/2} kg^{1/2} m^{3/2}$), and high-frequency parameter, K_{high} ($s^{-1} kg^{1/2} m^{3/2}$), respectively determine sensitivity at low and high frequencies. They are defined by the following equations:

$$K_{low} = h^2 \sqrt{\mu}, \quad (3)$$

$$K_{high} = \frac{1}{4} w^2 \sqrt{E}, \quad (4)$$
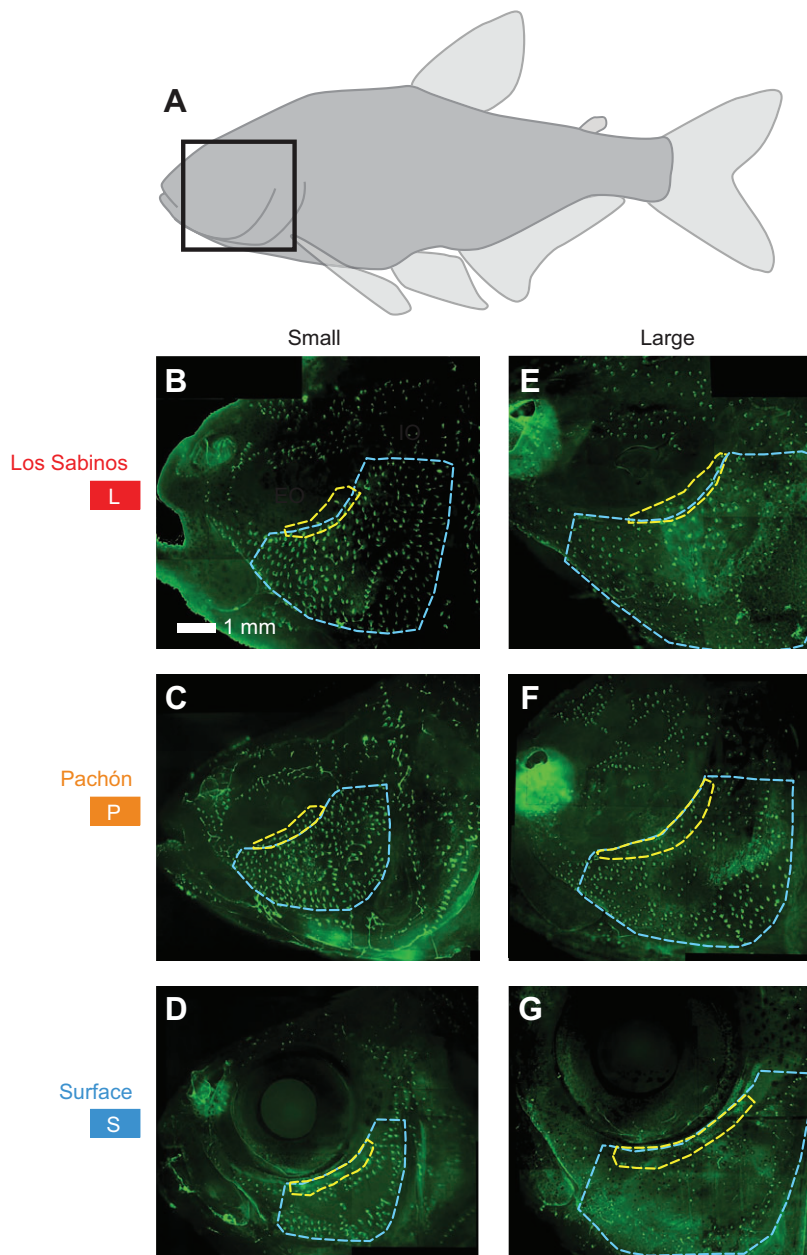
Fig. 6. The spatial distribution of superficial neuromasts.
(A) The cupulae of neuromasts were visualized with fluorescent microspheres in a cranial region (black square) for small (B–D) and large (E–G) adult fish from Los Sabinos (B,E) and Pachón (C,F) cavefish and sighted surface fish (D,G) populations. (B–G) For each group, the neuromasts around the eye orbit (EO, yellow dashed line) and in the infraorbital bone 3 regions (IO-3, blue dashed line) are highlighted.

where h is the cupula height, μ is the dynamic viscosity of water ($\mu=8.9\times10^{-4}$ Pa s), w is the cupula width and E is the Young's modulus of cupular material ($E=80$ Pa) (McHenry and van Netten, 2007). These parameters also determine the cut-off frequency for low-pass filtering, f_0 (Hz), as given by the following equation:

$$f_0 = \frac{1}{2}\left(\frac{K_{\text{low}}}{K_{\text{high}}}\right)^2 . \qquad (5)$$

For stimuli below this cut-off, the low-frequency sensitivity S_{low} (s) is given by:

$$S_{\text{low}} = K_{\text{low}} K_{\text{comp}} \sqrt{2f} . \qquad (6)$$

For stimuli that exceed the cut-off frequency, sensitivity S_{high} (s) is invariant with the stimulus frequency and defined by the following equation:

$$S_{\text{high}} = K_{\text{high}} K_{\text{comp}} . \qquad (7)$$

Vibration attraction behavior

Blind cavefish are attracted to fluid oscillations in a manner that varies with stimulus frequency. As previously established (Yoshizawa et al.,

2010), this behavior may be characterized by recording how frequently fish approach a vibrating rod that generates waves. We conducted measurements of VAB after an acclimation period (4 or 5 days), where fish were placed in a cylindrical assay chamber (Pyrex 325 ml glass dish, 10 cm diameter×5 cm high; Corning, Corning, NY, USA) with water filled to a height of 30–35 mm. Fluid oscillations were created using a 7.5 mm diameter glass rod inserted at a depth of 15–18 mm below the surface of the water. The rod was supported by a transparent plastic plate (1 mm thick×95 mm long). This rod was vibrated with a function generator (model LG1301, Leader Instruments Corp., Cypress, CA, USA) driving an audio speaker (Pro Speakers, Apple, Cupertino, CA, USA). Vibration was calibrated for 5–500 Hz, with the amplitude ranging from 0.02 to 1.52 mm by a high-speed CCD camera, as described previously (Yoshizawa et al., 2010). A fish was video-recorded for a 3 min period under the illumination of an infrared light (880 nm wavelength, BL41192-880 black light, Advanced Illumination, Rochester, VT, USA). An infrared CCD camera (Qicam IR, Qimaging, Surrey, BC, Canada) with a zoom lens (Zoom 7000, Navitar, Rochester, NY, USA) was used to capture images at 10 frames s^{-1} using StreamPix 3.36.0 video recording software (NorPix, Montreal, QC, Canada). The distance between the glass rod and the center
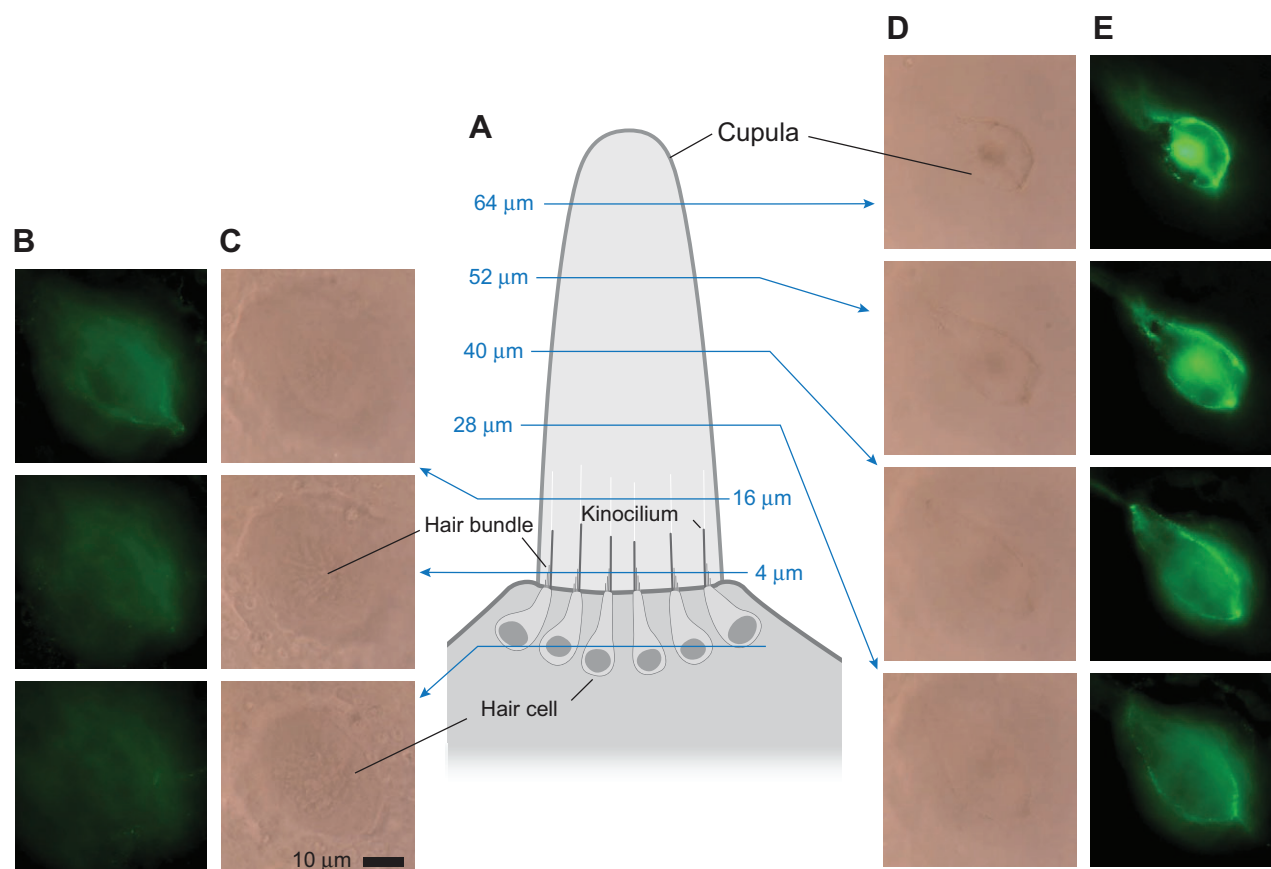
Fig. 7. Neuromast morphology was visualized with a compound microscope using two methods of illumination for a single IO-3 neuromast. (A) The major anatomical features of a neuromast are illustrated schematically for a side-view of the neuromast, which highlights the extracellular cupula and hair cells, each of which includes a hair bundle. (B–E) Optical planes (at 12 µm intervals, blue lines) focused through the height of the neuromast revealed the hair cells, under DIC illumination (C,D) and the peripheral shape of the cupula, which appeared with the greatest contrast under fluorescence illumination (B,E). The position of each optical section is defined relative to the apical surface of the sensory epithelium at the base of the cupula.

position of the fish was analyzed using the Tracker plugin for ImageJ 1.35s software (NIH, Bethesda, MD, USA).

Statistical analysis

Measurements of dependent variables were described by the median and quartile values. Outliers were identified as values that exceeded 50% of the range between the first and third quartiles. We used a three-factor ANOVA to test the effects of population (Los Sabinos, Pachón or surface fish), neuromast position (EO or IO-3) and age (small or large adults). The dependent variables in this analysis were the width, height and aspect ratio (height/width) of the neuromast cupula and its number of hair cells. We additionally tested four mechanical parameters (K_{comp}, K_{low}, K_{high} and f_0) that were calculated (Eqns 2–4) from morphometric parameters. In the event of a significant effect of population or an interaction between factors, we performed Dunn–Sidak *post hoc* comparisons between groups to determine the cause of variation (Sokal and Rohlf, 1995). The same approach was applied to examine differences in behavior and mechanical sensitivity to a 35 Hz stimulus. All data analyses were performed with custom-written Matlab programs (v2012b; MathWorks, Natick, MA, USA).

Author contributions
M.Y. and M.J.M. designed the study, wrote the manuscript and collaborated on data acquisition and analysis. All experiments were performed by M.Y. S.M.v.N. developed the analytical model and W.R.J. and S.M.v.N. provided tools and reagents for the experiments. S.M.v.N. and W.R.J. provided input on the manuscript.

References
Bleckmann, H., Breithaupt, T., Blickhan, R. and Tautz, J. (1991). The time course and frequency content of hydrodynamic events caused by moving fish, frogs, and crustaceans. *J. Comp. Physiol. A* **168**, 749-757.

Bradic, M., Beerli, P., García-de León, F. J., Esquivel-Bobadilla, S. and Borowsky, R. L. (2012). Gene flow and population structure in the Mexican blind cavefish complex (*Astyanax mexicanus*). *BMC Evol. Biol.* **12**, 9.

Coombs, S., Görner, P. and Münz, H. (1989). *The Mechanosensory Lateral Line*. New York, NY: Springer-Verlag.

Dinklo, T. (2005). Mechno- and electrophysiological studies on cochlear hair cells and superficial lateral line cupulae. Neurobiophysics Doctoral Dissertation, University of Groningen, Netherlands.

Dowling, T. E., Martasian, D. P. and Jeffery, W. R. (2002). Evidence for multiple genetic forms with similar eyeless phenotypes in the blind cavefish, *Astyanax mexicanus*. *Mol. Biol. Evol.* **19**, 446-455.

Gallo, N. D. and Jeffery, W. R. (2012). Evolution of space dependent growth in the teleost *Astyanax mexicanus*. *PLoS ONE* **7**, e41443.

Géléoc, G. S. G., Lennan, G. W. T., Richardson, G. P. and Kros, C. J. (1997). A quantitative comparison of mechanoelectrical transduction in vestibular and auditory hair cells of neonatal mice. *Proc. Biol. Sci.* **264**, 611-621.

Gross, J. B. (2012). The complex origin of *Astyanax cavefish*. *BMC Evol. Biol.* **12**, 105.

Hudspeth, A. J. (1982). Extracellular current flow and the site of transduction by vertebrate hair cells. *J. Neurosci.* **2**, 1-10.

Jeffery, W. R. (2001). Cavefish as a model system in evolutionary developmental biology. *Dev. Biol.* **231**, 1-12.

Jeffery, W. R. (2009). Chapter 8. Evolution and development in the cavefish *Astyanax*. *Curr. Top. Dev. Biol.* **86**, 191-221.

Jeffery, W. R. and Martasian, D. P. (1998). Evolution of eye regression in the cavefish *Astyanax*: apoptosis and the Pax-6 gene. *Am. Zool.* **38**, 685-696.

Lang, H. H. (1980). Surface wave discrimination between prey and nonprey by the backswimmer *Notonecta glauca* L. (Hemiptera, Heteroptera). *Behav. Ecol. Sociobiol.* **6**, 233-246.

McHenry, M. J. and van Netten, S. M. (2007). The flexural stiffness of superficial neuromasts in the zebrafish (*Danio rerio*) lateral line. *J. Exp. Biol.* **210**, 4244-4253.

McHenry, M. J., Strother, J. A. and van Netten, S. M. (2008). Mechanical filtering by the boundary layer and fluid-structure interaction in the superficial neuromast of the fish lateral line system. *J. Comp. Physiol. A* **194**, 795-810.

Menuet, A., Alunni, A., Joly, J. S., Jeffery, W. R. and Rétaux, S. (2007). Expanded expression of Sonic Hedgehog in *Astyanax* cavefish: multiple consequences on forebrain development and evolution. *Development* **134**, 845-855.

Mitchell, R. W., Russell, W. H. and Elliott, W. R. (1977). *Mexican Eyeless Characin Fishes, Genus Astyanax: Environment, Distribution and Evolution.* Lubbock, TX: Texas Tech University Press.

Ornelas-García, C. P., Domínguez-Domínguez, O. and Doadrio, I. (2008). Evolutionary history of the fish genus *Astyanax* Baird and Girard (1854) (Actinopterygii, Characidae) in Mesoamerica reveals multiple morphological homoplasies. *BMC Evol. Biol.* **8**, 340.

Rohner, N., Jarosz, D. F., Kowalko, J., Yoshizawa, M., Jeffery, W. R., Borowsky, R. L., Lindquist, S. and Tabin, C. J. (2013). Cryptic variation in morphological evolution: HSP90 as a capacitor for the adaptive loss of eyes in cavefish. *Science* **342**, 1372-1375.

Schemmel, C. (1967). Vergleichende untersuchungen an den hautsinnesorganen ober- und unterirdisch lebender *Astyanax* Formen. *Zeitschrift für Morphologie der Tiere* **61**, 255-316.

Sokal, R. R. and Rohlf, F. J. (1995). *The Principles and Practice of Statistics in Biological Research.* New York, NY: W. H. Freeman and Company.

Teyke, T. (1988). Flow field, swimming velocity and boundary layer: parameters which affect the stimulus for the lateral line organ in blind fish. *J. Comp. Physiol. A* **163**, 53-61.

Teyke, T. (1990). Morphological differences in neuromasts of the blind cave fish *Astyanax hubbsi* and the sighted river fish *Astyanax mexicanus*. *Brain Behav. Evol.* **35**, 23-30.

van Netten, S. M. and Kroese, A. B. (1987). Laser interferometric measurements on the dynamic behaviour of the cupula in the fish lateral line. *Hear. Res.* **29**, 55-61.

van Netten, S. M. (2013). The biophysics of the fish lateral line. In *The Lateral Line. Springer Handbook of Auditory Research 48* (ed. S. Coombs), doi 10.1007/2506_2013_14. New York, NY: Springer.

Van Trump, W. J. and McHenry, M. J. (2008). The morphology and mechanical sensitivity of lateral line receptors in zebrafish larvae (*Danio rerio*). *J. Exp. Biol.* **211**, 2105-2115.

Webb, J. (1989). Developmental constraints and evolution of the lateral line system in teleost fishes. In *The Mechanosensory Lateral Line: Neurobiology And Evolution* (ed. S. Coombs, P. Gorner and H. Munz), pp. 79-97. New York, NY: Springer.

Wilkens, H. (1988). Evolution and genetics of epigean and cave *Astyanax fasciatus* (Characidae, Pisces) – support for the neutral mutation theory. *Evol. Biol.* **23**, 271-367.

Yamamoto, Y. and Jeffery, W. R. (2000). Central role for the lens in cave fish eye degeneration. *Science* **289**, 631-633.

Yamamoto, Y., Espinasa, L., Stock, D. W. and Jeffery, W. R. (2003). Development and evolution of craniofacial patterning is mediated by eye-dependent and -independent processes in the cavefish *Astyanax*. *Evol. Dev.* **5**, 435-446.

Yoshizawa, M. and Jeffery, W. R. (2008). Shadow response in the blind cavefish *Astyanax* reveals conservation of a functional pineal eye. *J. Exp. Biol.* **211**, 292-299.

Yoshizawa, M., Gorički, S., Soares, D. and Jeffery, W. R. (2010). Evolution of a behavioral shift mediated by superficial neuromasts helps cavefish find food in darkness. *Curr. Biol.* **20**, 1631-1636.

Yoshizawa, M., Ashida, G. and Jeffery, W. R. (2012a). Parental genetic effects in a cavefish adaptive behavior explain disparity between nuclear and mitochondrial DNA. *Evolution* **66**, 2975-2982.

Yoshizawa, M., Yamamoto, Y., O'Quin, K. E. and Jeffery, W. R. (2012b). Evolution of an adaptive behavior and its sensory receptors promotes eye regression in blind cavefish. *BMC Biol.* **10**, 108.

Yoshizawa, M., O'Quin, K. E. and Jeffery, W. R. (2013). QTL clustering as a mechanism for rapid multi-trait evolution. *Commun. Integr. Biol.* **6**, e24548.